

Supporting Information

Monolayer and Bilayer Graphene on Ru(0001): Layer-Specific and Moiré-Site-Dependent Phonon Excitations

Johannes Halle, Nicolas Néel, and Jörg Kröger
Institut für Physik, Technische Universität Ilmenau, D-98693 Ilmenau, Germany

I. DEFECTS OF MLG AND BLG ON RU(0001)

Figure 1 of the main article shows a representative overview STM image of MLG and BLG on Ru(0001). A few defects can be discerned, which are described in more detail here. In MLG missing mounds of the moiré pattern occur. They were previously observed and assigned to Ru(0001) vacancies [1]. They are not due to defects in the graphene lattice because atomically resolved STM images of MLG reveal that structurally intact graphene covers sites of missing moiré mounds.

Missing mounds in STM images of the BLG moiré pattern are related to the graphene–Ru(0001) interface because of the structural integrity of the top graphene sheet. They may occur due to carbidic surface structures [2] or imperfect C patches [3] in the course of C segregation from the Ru bulk, which then lead to a local imperfect stacking of the graphene layers.

Other defects show up as faint protrusions on both MLG and BLG with a variety of lateral extents. They are typical for a freshly prepared Ru(0001) surface, Figure S1, and are most likely due to genuine bulk impurities, such as C.

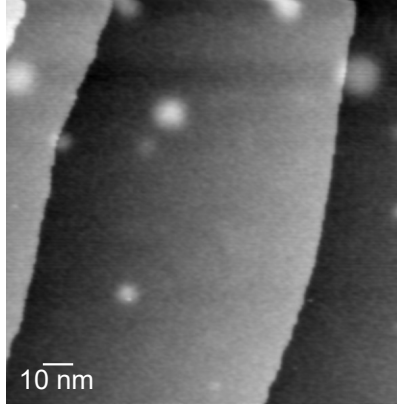


FIG. S1. STM image of freshly prepared Ru(0001) (0.2 V, 100 pA, 130 nm \times 130 nm). Bright protrusions with different lateral extents are most likely due to genuine bulk impurities.

II. CALCULATION OF TWIST ANGLES

Twist angles enclosed by stacked layers can only be indirectly inferred by measuring the angle between the moiré lattice and the atomically resolved graphene lattice. Figure S2a shows the directions of the moiré pattern (\mathbf{m}) and the graphene lattice (\mathbf{g}), which enclose an angle α . Defining reciprocal lattice vectors of the moiré pattern, $k_m = 2\pi/a_m$, the graphene lattice, $k_g = 2\pi/a_g$, and the Ru(0001) surface, $k_{Ru} = 2\pi/a_{Ru}$, with respective direct-lattice constants a_m , a_g and a_{Ru} the twist angle θ enclosed by graphene and Ru(0001) lattices reads (Figure S2b)

$$\cos \theta = \frac{k_g^2 + k_{Ru}^2 - k_m^2}{2k_g k_{Ru}} = \frac{a_g a_{Ru}}{2} \left(\frac{1}{a_g^2} + \frac{1}{a_{Ru}^2} - \frac{1}{a_m^2} \right). \quad (S1)$$

The triangle spanned by \mathbf{k}_m , \mathbf{k}_g and \mathbf{k}_{Ru} (Figure S2b) further shows that

$$\frac{k_m}{\sin \theta} = \frac{k_{Ru}}{\sin \alpha}. \quad (S2)$$

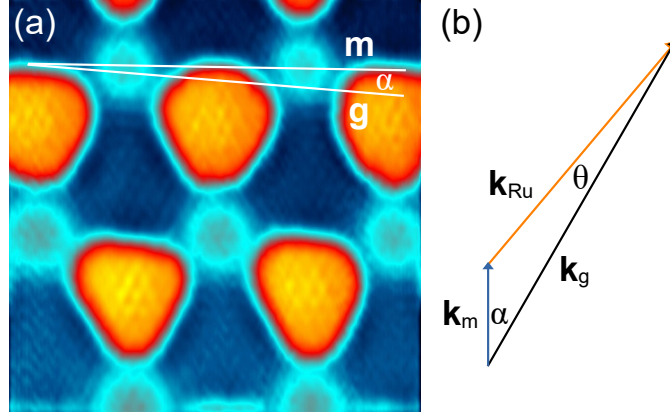


FIG. S2. (a) STM image of MLG on Ru(0001) with indicated orientations of the moiré pattern (**m**) and the atomically resolved graphene lattice (**g**), which enclose an angle α . (b) Reciprocal-vector diagram showing how the moiré reciprocal lattice vector \mathbf{k}_m results from the reciprocal lattice vectors of graphene, \mathbf{k}_g , and Ru(0001), \mathbf{k}_{Ru} . Angle θ denotes the twist angle between graphene and Ru(0001) lattices. The vector diagram is not to scale with the STM image for clarity reasons.

Consequently, variations in the moiré orientation $\Delta\alpha$ can be associated to changes in the twist angle $\Delta\theta$ according to

$$\Delta\alpha \approx \frac{k_{Ru}}{k_m} \Delta\theta \quad (\text{S3})$$

for small α and θ . Therefore, small changes in θ are magnified by a factor $k_{Ru}/k_m = a_m/a_{Ru}$. In order to match the uncertainty of the measured angle α , the accuracy margin of θ is small.

III. ZERO-BIAS RESONANCE IN d^2I/dV^2 SPECTRA

Common to all d^2I/dV^2 spectra is a peak centered at ≈ 0 V. Its line shape and signal strength depend on the actual tip used for spectroscopy. Importantly, the graphene phonon signatures remain invariant and are independent of the zero-bias feature. Figure S3 shows dI/dV spectra (α, β, γ) that were acquired atop v_α (α, β) and v_β (γ) sites of BLG on four different days with four different tips. The steplike variations of dI/dV (arrows in β) result from the graphene phonon excitation and are present in all spectra. For comparison, a numerically integrated spectrum resulting from the d^2I/dV^2 data set plotted in Figure 2e (v_α) of the main article was added to Figure S3 as spectrum δ . The right inset to Figure S3 shows a close-up view of the spectroscopic data in the vicinity of 0 V. The different evolution of the spectral data (α – δ) gives rise to the various zero-bias signatures visible in d^2I/dV^2 spectra.

In the course of tip preparation, field emission on and indentation into a Au substrate entails the modification of the tip apex. For instance, the resulting tip apex may be terminated by a Au_5 or a Au_4 pyramidal cluster (left inset to Figure S3). The electronic structure of such small clusters can change strongly upon modifying the atomic geometry [4]. Moreover, the orbital character in the vacuum depends on the balance of contributions of atomic states [5]. A low-energy vibrational excitation of the terminating Au atom may likewise contribute to the zero-bias peak. Such vibrational quanta were previously demonstrated to depend on the local atomic environment, too [6]. In order to identify the origin of the resonance close to 0 V, however, a systematic analysis comprising different tip materials and controllably terminated tips is required.

IV. SPATIAL VARIATION OF THE ELECTRON-PHONON COUPLING

In a combined experimental and theoretical study of graphene phonons using STM-IETS, the change in $g \equiv dI/dV$ due to the excitation of a phonon by an inelastic tunneling electron was determined as [7]

$$\frac{\Delta g}{g(0)} \propto \frac{\lambda^2}{\Gamma_\pi} \quad (\text{S4})$$

with $g(0) = dI/dV|_{V=0\text{V}}$, Γ_π the hybridization strength of graphene π -states with the electronic structure of the metal substrate and λ the electron-phonon coupling parameter of graphene. The relative signal change $\Delta g/g(0)$ is therefore

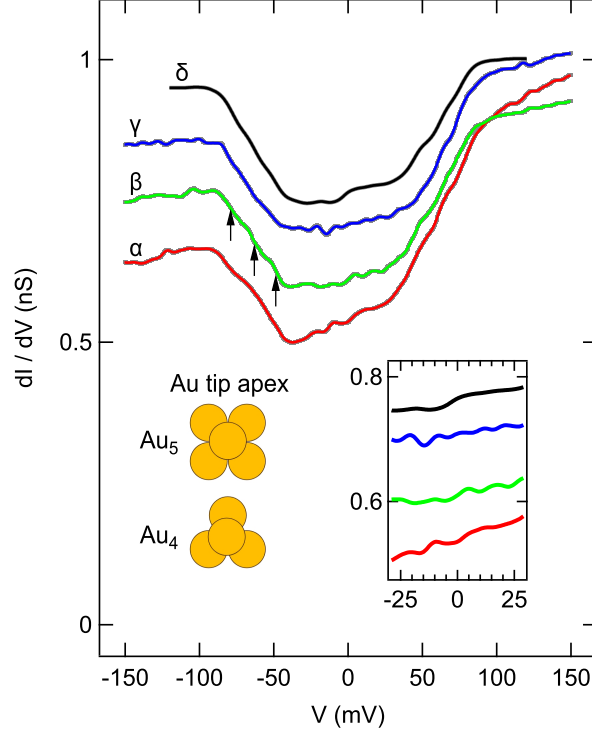


FIG. S3. Spectra of dI/dV acquired with different Au tips on v_α (α), v_β (β) and v_γ (γ) sites of independent BLG-covered Ru(0001) samples (feedback loop parameters: 150 mV, 100 pA, 20 mV_{pp}, 440 Hz). Spectrum δ is the numerical integration of the d^2I/dV^2 spectrum depicted in Figure 2e of the main article. Right inset: Close-up view of α - δ in the range $-29 \text{ mV} \leq V \leq 29 \text{ mV}$. Left inset: Sketch of Au clusters that possibly terminate the tip apex.

controlled by Γ_π , which due to the moiré corrugation of graphene varies spatially. Likewise, the observed spatial dependence of $\Delta g/g(0)$ may reflect the variation of λ with the actual spectroscopy site. The electron-phonon coupling parameter is intimately related to the electronic structure and the displacement pattern of the relevant phonon. The electronic structure of MLG on Ru(0001) changes locally, as exposed in the main article, which entails local variations of λ , too. A similar argument was put forward to explain the spatial dependence of a graphene optical phonon observed in STM-IETS previously [8].

-
- [1] J. Lu, A. C. Neto, and K. P. Loh, Nat. Commun. **3**, 823 (2012).
 - [2] F. Jiménez-Villacorta, L. Álvarez-Fraga, J. Bartolomé, E. Climent-Pascual, E. Salas-Colera, M. X. Aguilar-Pujol, R. Ramírez-Jiménez, A. Cremades, C. Prieto, and A. de Andrés, J. Mater. Chem. C **5**, 10260 (2017).
 - [3] M. Papagno, D. Pacilé, D. Topwal, P. Moras, P. M. Sheverdyaeva, F. D. Natterer, A. Lehnert, S. Rusponi, Q. Dubout, F. Calleja, E. Frantzeskakis, S. Pons, J. Fujii, I. Vobornik, M. Grioni, C. Carbone, and H. Brune, ACS Nano **6**, 9299 (2012).
 - [4] H. Häkkinen, Chem. Soc. Rev. **37**, 1847 (2008).
 - [5] P. Ferriani, C. Lazo, and S. Heinze, Phys. Rev. B **82**, 054411 (2010).
 - [6] S. D. Borisova, S. V. Eremeev, G. G. Rusina, V. S. Stepanyuk, P. Bruno, and E. V. Chulkov, Phys. Rev. B **78**, 075428 (2008).
 - [7] J. Halle, N. Néel, M. Fonin, M. Brandbyge, and J. Kröger, Nano Lett. **18**, 5697 (2018).
 - [8] A. Castellanos-Gomez, G. Rubio-Bollinger, S. Barja, M. Garnica, A. L. Vázquez de Parga, R. Miranda, and N. Agrait, Appl. Phys. Lett. **102**, 063114 (2013).